

In-Silico Study on the Role of Epstein Barr Virus to Translocate Tobacco Constituents into Blood to Lead to Oral Cancer

M. Dheer¹, A. Angel^{1*}, V. Joshi¹, S. Mohammed Buvvaji¹, B. Angel¹, H. Sawhney², R. Saxena³, N. Singh¹, B. Sharma¹, K. Kumari¹, A. Chitransh¹ and P. Sharma¹

¹Centre of Excellence in Virology & Immunology, Sharda University, Greater Noida, Uttar Pradesh, India-201310

²Sharda School of Dental Sciences, Sharda University, Greater Noida, Uttar Pradesh, India-201310

³Sharda School of Medical Sciences and Research, Sharda University, Greater Noida, Uttar Pradesh, India-201310

Tobacco contains more than 7000 compounds, out of which 69 are harmful which may lead to various types of cancer. Of these, N- nitrosamine, nicotine and Tar have been reported to reactivate Epstein-Barr virus from its latent phase to lytic phase and cause oral cancer. However, the exact mechanism in this reactivation is not fully known. Present paper focuses on interaction between tobacco ingredients with the EBV proteins using In-silico tools. From Protein Data Bank database, the structures were deduced and then docked to check binding affinities. We observed that interaction of nicotine with EBV early proteins rta (BRLF) and zta (BZLF) showed good score of -5.3 and -3.3 respectively while that between nitrosamine and rta and zta proteins, showed score of -2.9 and -2.7 respectively. Normally, the local physiological and innate immune system will resist the tobacco compounds to enter across oral mucosa and epithelial cells to cause further damage to the blood chemistry. However, these scores indicate possibility of translocation of carcinogenic compounds into blood, specifically among tobacco chewers who are infected by EBV. Our studies show that EBV interaction will help evade innate oral immunological resistance and thus infected people who are tobacco eaters will be prone to cancer.

Keywords: Oral cancer; BRLF; BZLF; Epstein Barr Virus; Nicotine; Nitrosamine

I. INTRODUCTION

Epstein - Barr Virus (EBV) is an oncogenic virus which is associated with the Oral and Nasopharyngeal Cancer. According to global burden, 265 000 cases of cancer and 164 000 deaths were reported to be infected by EBV (Khanet *et al.*, 2020). Also, around 90% of the population is infected with this virus worldwide (Cohen *et al.*, 2011). The virus belongs to the Gamma herpes virus family 4 and has a linear double-stranded DNA virus with more than 85 genes. It infects the Epithelial cell and the B lymphocyte cell and undergoes lytic as well as latent replication cycle within target cells. While latency mainly occurs in B lymphocytes, the lytic cycle occurs in oropharyngeal epithelial cells (Hadinoto *et al.*, 2009). The virus identifies CD21 receptor protein of B

lymphocytes, infects the B cells and disseminates infection to entire body through the circulating B cells.

There are many Open Reading Frames present in the virus, the major one encodes for 10 latent and 22 lytic cycle genes (3 Immediate Early genes, 10 Early genes and 9 late genes (IARC working group, 2012). Of these, the Zta (BZLF1) and rta (BRLF1) are immediate early genes which code for viral transcriptional activator proteins (ZEBRA protein coded by BZLF1) that bind with the nucleotide-specific promoter region (OriLyt) and lead to reactivation of EBV from latent to lytic phase (Ward *et al.*, 2022). This reactivation further leads to uncontrolled cell growth, cell proliferation, oncogenesis and apoptosis (Germini *et al.*, 2020). The protein coded by BRLF1 gene also reactivates lytic cycle from latency in B cells and downregulates apoptosis and activates interferon secretion by T helper cells specifically

*Corresponding author's e-mail: annetteangel156@gmail.com

IFNB1 (Interferon beta 1), IRF3 (Interferon regulatory factor 3) and IRF7 (Interferon regulatory factor 7).

The combination of EBV and Tobacco may thus increase the risk towards oral cancer (Han *et al.*, 2019). Tobacco further increases ROS (Reactive oxygen species) that causes the oxidative stress leading to cell damage. Our In-Silico studies have shown a good binding between carcinogenic ingredients of tobacco and viral proteins which strengthens the combination of EBV and tobacco as the cancer-causing cascade among EBV patients and tobacco chewers. The present paper reports the details of work accomplished.

II. MATERIALS AND METHOD

The present study was conducted using in-silico tools to firstly identify the possibility of interactions. In tobacco, (smoke and smokeless forms) thousands of chemicals are available, out of which 69 are toxic and carcinogenic. These include cadmium, nickel, formaldehyde, arsenic, polycyclic (such as benzopyrene) tobacco-specific nitrosamines, phenols, Nicotine and Tar, which are known to cause cancer (National Toxicology Prog, 2016; Zhao *et al.*, 2020). After a thorough literature search, two important constituents which were present in maximum concentration were selected, Nitrosamine and Nicotine. The Alpha fold 2 protein structure prediction software was used to deduce the two structure and then Chimera Autock Vina software was used to see their interaction with the two EBV proteins. The zta and rta sequence was retrieved from the NCBI database and then further using the Protein Data Bank (PDB) database, the protein structure was retrieved.

III. RESULTS AND DISCUSSION

The protein sequences of rta and zta used was uniprot kB/swiss prot:P03209.1 and 7NX5 respectively and the structure of both these are displayed in Figure 1. Figure 1(A) represents the Cartoon model of zta protein depicted by varied colours; orange to blue and Figure 1(B) shows the Model representation with hydrophobic surfaces. The Hydrophobic residue is coloured yellow-brown, while hydrophilic residue is pale blue.

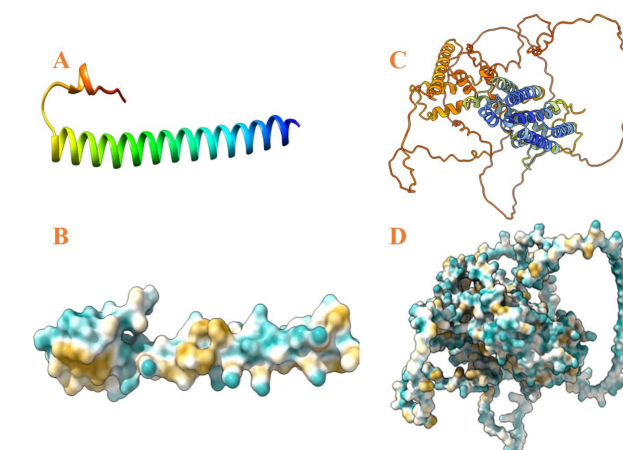


Figure 1. zta protein structure (A: Cartoon model; B: Hydrophobic structure) and rta protein structure (C: Cartoon model; D: Hydrophobic structure).

Figure 1(C) shows Cartoon model of the rta protein in varied colours orange to blue. Orange indicates high confidence while blue area indicates low confidence. Figure 1(D) shows Model representation with hydrophobic surfaces, the hydrophobic residue is coloured yellow-brown, while hydrophilic residue is pale blue.

The CID (Compound Identifier) of ligands (Tobacco compounds) were downloaded from the PubChem online server (Figure 2). The molecular weight of Nicotine (CID-89594) (chemical formula: $C_{10}H_{14}N_2$) is 162.23 g/mol and that of Nitrosamine (CID-37183) (chemical formula: H_2N_2O) is 46.029 g/mol. Both were found to have high penetration into cells. Their molecular structure (SDF file) was downloaded from PubChem database and then 3D structure derived.

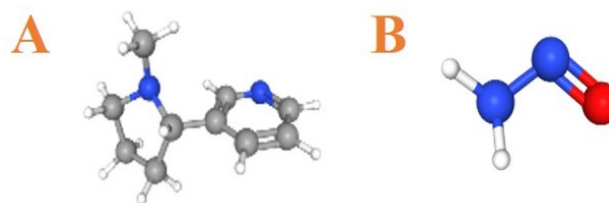


Figure 2. Structure of Nicotine (A) and Nitrosamine (B) as downloaded from PubChem server.

The Figure 3 shows the Test score for each Position's Predicted Local Distance Difference (PLDDT). Five models of zta were predicted using Alpha fold 2 software. The location of the amino acid can be confidently predicted when values between 70 and 90 display excellent accuracy. When

PDDLDT is larger than 90, the precision is quite high and is comparable to empirically verified structure. It is likely that the structure is accurate, even though a result between 50 and 70 denotes a lower accuracy.

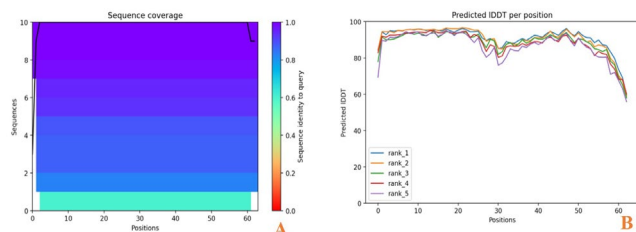


Figure 3. Predicted local distance test (pLDDT) plotted graph of zta protein.

The Figure 4 shows Predicted Aligned Error (PAE) score models of Rank 1, 2, 3, 4, and 5. For each pair of residues, this score shows the estimated errors of expected distance. Each amino acids' location is indicated on both axes. The colour coding for the distance between two amino acids ranges from blue to red.

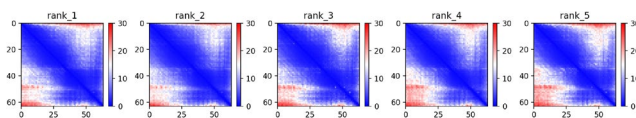


Figure 4. Error plot graph of zta protein.

The Figure 5 shows test score for each PLDDT. Five model of rta protein were predicted using Alpha fold 2 software. Value falls between 70 and 90 proteins is confidentially predicted and display excellent accuracy. When PDDLDT value falls above 90, the accuracy is very excellent and is comparable to experimentally verified structure. The values that fall between 50 and 70 denotes very low accuracy. In the PDDLDT of rta, the starting value fall between 30-90, which is quite good, but the later values are falling between 20-40 which denotes low accuracy.

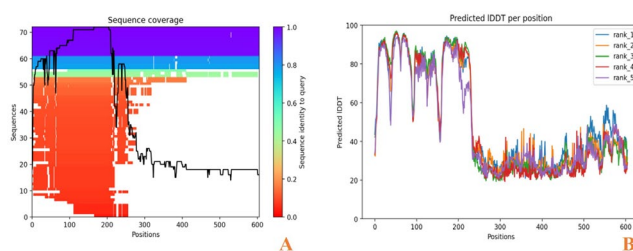


Figure 5. Predicted Local Distance Test (PLDDT) Plotted Graph of rta Protein.

The Figure 6 displays PAE score models of Rank 1, 2, 3, 4, and 5. For each pair of residues, this score shows the estimated errors of expected distance. Each amino acid's location is indicated on both axes. The colour coding for the distance between two amino acids range from blue to red.

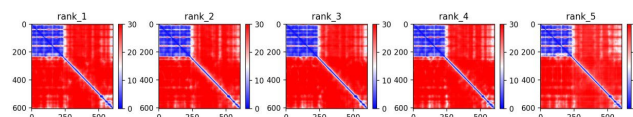


Figure 6. Error plot graph of rta protein.

Figure 7 represents Ramachandran plotted graph of zta and rta proteins. Figure 7(A) displays the energetically permitted regions for amino acid residues' backbone dihedral angles ψ against ϕ in the zta structure. The ϕ -angle is formed by the bond between $C\alpha$ and N atom. The ψ angle is formed by the bond between $C\alpha$ and C atom of the peptide. The favoured, allowed, "generously allowed," and unallowed zones are represented by the colours red, brown, dark yellow, and light yellow, respectively.

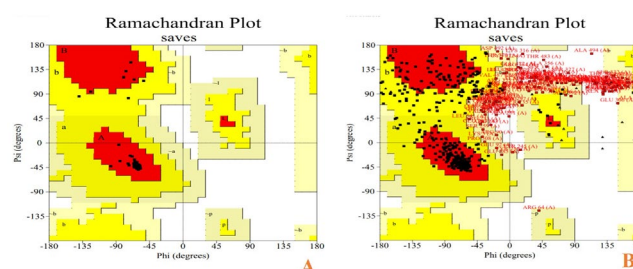


Figure 7. Ramachandran plotted graph of zta protein (A) and rta protein (B).

Figure 7(B) displays the energetically permitted regions for amino acid residues' backbone dihedral angles ψ against ϕ in the rta structure. The ϕ -angle is formed by the bond between $C\alpha$ and N atom. The ψ angle is formed by the bond

between C α and C atom of the peptide. The favoured, allowed, "generously allowed," and unallowed zones are represented by the colours red, brown, dark yellow, and light yellow, respectively.

Next, the Protein (zta and rta) and the ligands (Nitrosamine and Nicotine) were prepared for docking studies. With the help of Chimeric autodock vina the missing polar hydrogen molecules were added and the overall charge was neutralised using the standard residues AMBER ff14SB (Figure 8 and 9). The interaction between nicotine and rta (BRLF) was seen at different position of amino acids Arginine (108), Tyrosine (109), Glutamine (204), Glycine (207), Threonine (208), Leucine (231) under the score of -5.3, which indicates high affinity. The interaction between nicotine and zta (BZLF) was seen at different position of amino acids i.e. Asparagine (09), Arginine (10), Serine (13), Arginine (14), Arginine (17) under the score of -3.3, which indicates high affinity (Figure 8, Table 1).

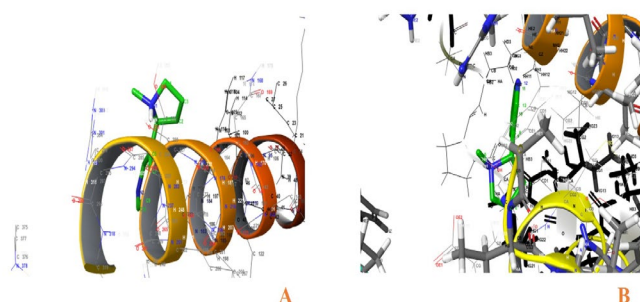


Figure 8. Docking result of Nicotine with zta (A) and rta (B) proteins.

Table 1. Docking score of Nicotine with rta and Zta

S.No.	Nicotine and rta			Nicotine and Zta		
	Score	RMD l.b	RMSD u.b.	Score	RMD l.b	RMSD u.b.
1	-5.3	1.957	2.851	-3.3	2.927	5.123
2	-5.3	11.764	12.646	-3.3	0.906	4.508
3	-5.2	10.832	11.713	-3.2	3.135	4.039
4	-5.2	10.75	12.173	-3.1	3.325	4.404
5	-5.1	1.575	1.971	-3.1	1.783	4.003
6	-5.0	12.439	13.347	-3.0	6.608	8.004
7	-4.9	15.719	18.20	-2.9	2.521	4.022

8	-4.9	2.25	3.86	-2.9	5.971	8.028
---	------	------	------	------	-------	-------

The interaction between nitrosamine and rta (BRLF) was seen at different position of amino acids, Proline (03), Asparagine (85) under the score of -2.9, which indicates high affinity. The interaction between nitrosamine and zta (BZLF) was seen at different position of amino acids Threonine (61), Arginine (60) under the score of -2.7, which indicates high affinity (Figure 9, Table 2).

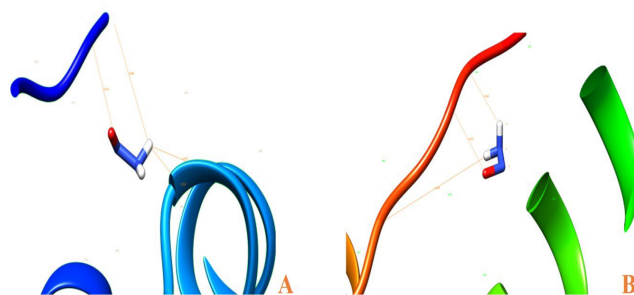


Figure 9. Docking result of Nitrosamine with rta (A) and zta (B) proteins.

Table 2. Docking score of Nitrosamine with rta and Zta

S.No.	Nitrosamine and rta			Nitrosamine and Zta		
	Score	RMD l.b	RMSD u.b.	Score	RMD l.b	RMSD u.b.
1	-2.9	12.631	12.818	-2.7	1.67	2.041
2	-2.8	27.259	27.579	-2.7	3.047	3.047
3	-2.7	33.872	33.959	-2.6	1.812	1.812
4	-2.7	38.936	38.959	-2.5	8.163	8.163
5	-2.6	9.451	9.629	-2.4	4.761	4.799
6	-2.6	36.326	36.487	-2.3	2.569	2.595
7	-2.6	31.587	31.758	-2.1	31.71	31.731
8	-2.6	36.671	36.696	-1.9	32.002	32.007

Since past five decades, Epstein Barr Virus has demonstrated to be the most common tumorigenic virus causing various cancers such as Burkitts lymphoma, Hodgkins's lymphoma, natural killer/T-cell lymphoma, nasopharyngeal carcinoma and gastric carcinoma. Its two immediate early proteins; rta (BRLF1) and zta (BZLF1) are responsible for reactivation (Guidry & Birdwell, 2018) from latent to lytic phase in B cells which then causes these cancers.

Though it has been reported that 90% of the population carries this virus yet initiating or triggering of the

tumorigenic factors have not been studied fully. Interaction towards this tumour formation. Tobacco is coincidentally a major etiological factor for causing head, neck and lung cancer (Pemberton, 2018). According to W.H.O., 8 million deaths per year are recorded due to tobacco all over the world (7 million deaths due to smoking tobacco and 1.3 million due to smokeless tobacco). Smokeless form is most prevalent in our country India. The products of smokeless tobacco are Gutka, chaini khaini, zarda, and betel quid while Bidi, cigarette, cigar, and hookah are the smoking tobacco products. Tobacco is known to cause epigenetic alteration of oral epithelial cell keratinocytes (Jian *et al.*, 2019). The tendency of oral cancer development due to tobacco consumption is well understood. Primary component of tobacco that makes human addicted to it is, nicotine. Although the role of Nicotine in cancer causation is not well understood but one study has reported that it induces DNA

of chemicals or toxins can be one of the possible enhancers damage (Hecht, 2002; Hecht & Hatsukami, 2022). Another potent compound is Nitrosamine which in in-vitro studies has shown some morphological changes of the cell (Fang *et al.*, 2010).

IV. CONCLUSION

Our In-Silico studies have shown good binding affinity of both these compounds with the two proteins rta and zta of the EBV. Also, it was seen that transmembrane translocation of Nitrosamine is more due to its low molecular weight and hence can activate these proteins. These proteins generally bind with the EBV DNA and enhances replication of the viral genome. We conclude that presence of nitrosamine and nicotine in good amount may lead to activation of EBV in the epithelial cells of the oral cavity at a much early stage which otherwise would have remained inactive.

V. REFERENCES

- Cohen, JI, Fauci, AS, Varmus, H & Nabel, GJ 2011, 'Epstein-Barr virus: an important vaccine target for cancer prevention', *Science Translational Medicine*, vol. 3, no. 107, p. 107fs7.
- Fang, CY, Lee, CH, Wu, CC, Chang, YT, Yu, SL, Chou, SP, Huang, PT, Chen, CL, Hou, JW, Chang, Y, Tsai, CH, Takada, K & Chen, JY 2009, 'Recurrent chemical reactivations of EBV promotes genome instability and enhances tumor progression of nasopharyngeal carcinoma cells', *International Journal of Cancer*, vol. 124, no. 9, pp. 2016–2025.
- Germini, D, Sall, FB, Shmakova, A, Wiels, J, Dokudovskaya, S, Drouet, E & Vassetzky, Y 2020, 'Oncogenic Properties of the EBV ZEBRA Protein', *Cancers*, vol. 12, no. 6, p. 1479.
- Guidry, JT, Birdwell, CE & Scott, RS 2018, 'Epstein-Barr virus in the pathogenesis of oral cancers', *Oral Diseases*, vol. 24, no. 4, pp. 497–508.
- Hadinoto, V, Shapiro, M, Sun, CC & Thorley-Lawson, DA 2009, 'The dynamics of EBV shedding implicate a central role for epithelial cells in amplifying viral output', *PLoS Pathogens*, vol. 5, no. 7, p. e1000496.
- Han, H, Huang, W, Du, W, Shen, Q, Yang, Z, Li, MD & Chang, SL 2019, 'Involvement of Interferon Regulatory Factor 7 in Nicotine's Suppression of Antiviral Immune Responses', *Journal of Neuroimmune Pharmacology*, vol. 14, no. 4, pp. 551–564.
- Hecht, SS 2002, 'Cigarette smoking and lung cancer: chemical mechanisms and approaches to prevention', *Lancet Oncology*, vol. 3, pp. 461–469.
- Hecht, SS & Hatsukami, DK 2022, 'Smokeless tobacco and cigarette smoking: chemical mechanisms and cancer prevention', *Nature Reviews Cancer*, vol. 22, pp. 143–155.
- IARC Working Group on the Evaluation of Carcinogenic Risks to Humans, Biological Agents, Lyon (FR): International Agency for Research on Cancer 2012, (IARC Monographs on the Evaluation of Carcinogenic Risks to Humans, no. 100B.) Epstein-Barr Virus, retrieved from <https://www.ncbi.nlm.nih.gov/books/NBK304353/>

- Jiang, X, Wu, J, Wang, J & Huang, R 2019, 'Tobacco and oral squamous cell carcinoma: A review of carcinogenic pathways', *Tobacco Induced Diseases*, vol. 17, p. 29.
- Khan, G, Fitzmaurice, C, Naghavi, M & Ahmed, LA 2020, 'Global and regional incidence, mortality and disability-adjusted life-years for Epstein-Barr virus-attributable malignancies, 1990-2017', *BMJ Open*, vol. 10, no. 8, p. e037505.
- National Toxicology Program, Tobacco-Related Exposures. In: Report on Carcinogens. Fourteenth Edition, US Department of Health and Human Services, Public Health Service, National Toxicology Program. 2016.
- networks', *Expert Systems with Applications*, vol. 46, no. C, pp. 139–144.
- Pemberton, M 2018, 'Oral cancer and tobacco: developments in harm reduction', *British Dental Journal*, vol. 225, pp. 822–826.
- Ward, BJH, Schaal, DL, Nkadi, EH & Scott, RS 2022, 'EBV Association with Lymphomas and Carcinomas in the Oral Compartment', *Viruses*, vol. 14, no. 12, p. 2700.
- Zhao, C, Xie, Y, Zhou, X, Zhang, Q & Wang, N 2020, 'The effect of different tobacco tar levels on DNA damage in cigarette smoking subjects', *Toxicology Research*, vol. 9, no. 3, pp. 302–307.